

## Sapriearine protects H9c2 cardiomyocytes against hypoxia/reoxygenation-induced apoptosis by activating Nrf2

Gang Zhang<sup>#</sup>, Dongying Zhang<sup>#</sup>, Xiwen Zhang, Kun Yu and Aixia Jiang<sup>✉</sup>

Department of Cardiology, The Affiliated Huaian No. 1 People's Hospital of Nanjing Medical University, Huaian, Jiangsu 223300, China

Myocardial infarction is a major cause of mortality and disability worldwide. Ischemia/reperfusion injury is the key factor that results in the increase in infarct size in pathogenesis. To find a novel therapy for myocardial infarction, we have evaluated sapriearine, a natural diterpenoid, using H9c2 cardiomyocytes injured by hypoxia/reoxygenation and explored the possible mechanisms. The results showed that sapriearine improved cell survival by increasing cell viability and blocking the release of lactate dehydrogenase. Meanwhile, sapriearine was found to attenuate mitochondrial dysfunction by inhibiting calcium overload, collapse of the mitochondrial membrane potential, and opening of the mitochondrial permeability transition pore. And oxidative stress resulting from hypoxia/reoxygenation was ameliorated by sapriearine through the reduction of reactive oxygen species and malondialdehyde as well as activation of superoxide dismutase and catalase. Additionally, sapriearine inactivated cysteinyl aspartate-specific proteinase-3, the up-regulated B-cell lymphoma-2 and down-regulated Bcl-2-associated X protein, to inhibit hypoxia/reoxygenation-induced apoptosis. Further research revealed sapriearine-activated nuclear factor E2-related factor-2 in H9c2 cardiomyocytes, which is closely associated with its protective effects. These findings can provide evidence for the discovery of new therapies targeting myocardial infarction and the application of sapriearine in clinical practice.

**Keywords:** sapriearine, myocardial infarction, H9c2 cardiomyocytes, apoptosis, Nrf2

**Received:** 15 September, 2021; revised: 22 October, 2021; accepted: 26 November, 2021; available on-line: 26 May, 2022

✉e-mail: [medxc63@sohu.com](mailto:medxc63@sohu.com)

<sup>#</sup>These authors contributed equally to this work.

**Abbreviations:** cl-2, B-cell lymphoma-2; Bax, Bcl-2-associated X protein; CAT, catalase; caspase-3, cysteinyl aspartate specific proteinase-3; Nrf2, nuclear factor E2-related factor-2; Keap1, Kelch-like ECH associated protein 1; LDH, lactate dehydrogenase; MDA, malondialdehyde; ROS, reactive oxygen species; SOD, superoxide dismutase

### INTRODUCTION

Myocardial infarction resulting from ischemia is one of the leading causes of death and disability worldwide (Thygesen *et al.*, 2012). Although timely myocardial reperfusion with thrombolytic therapy or primary myocardial intervention can reduce the size of the infarct and improve the clinical outcome, restoration of blood flow to the ischemic myocardium will induce the injury and result in cardiomyocyte apoptosis, as well as increase the size of the infarct (Yellon & Hausenloy, 2007). In the

pathogenesis of myocardial reperfusion injury, oxidative stress plays a central role, since overproduction of reactive oxygen species (ROS) causes calcium overload and leads to apoptosis of cardiomyocytes (Zhao, 2004). Therefore, targeting oxidative stress will provide a potential approach to attenuate myocardial reperfusion injury (Marczin *et al.*, 2003).

Nuclear factor E2-related factor-2 (Nrf2) is an important transcription factor that regulates the transcription of target genes encoding antioxidant enzymes by binding to the promoter region of these genes (Kaspar *et al.*, 2009). Under basal conditions, Nrf2 is sequestered in the cytosol by Kelch-like ECH associated protein 1 (Keap1) to facilitate ubiquitination and degradation by the 26S proteasome. However, under the induced condition, oxidants or electrophiles can interact with Keap1 and result in activation of Nrf2 and translocation into the nucleus of the cytosol to implement transcriptional regulation (Yamamoto *et al.*, 2018). As in a previous report, many antioxidant enzymes such as superoxide dismutase (SOD), catalase (CAT) are regulated by Nrf2 (Shaw & Chattopadhyay, 2020). Therefore, activation of Nrf2 can provide a potential therapeutic approach for the treatment of diseases related to oxidative stress, including myocardial ischemia and reperfusion injury (Shen *et al.*, 2019).

In the discovery of a new therapy for myocardial infarction, phytochemicals have played a crucial role (Kumar & Nayak, 2017). *Salvia* is a genus that belongs to the Lamiaceae family, and most plants in this genus are used for the treatment of various diseases, including cardiovascular disease. Especially *Salvia miltiorrhiza*, a member of this genus, has been used for the treatment of cardiovascular diseases for thousands of years in traditional Chinese medicine (Xu *et al.*, 2018). *Salvia prionitis* is another plant of the genus *Salvia*, which is used in Chinese folk medicine as an antiphlogistic, antibacterial, and antitubercular drug (Chen *et al.*, 2002). Phytochemical investigations have revealed there are diterpenoids, polyphenols, and alkaloids in this plant (Zhao *et al.*, 1996; Li *et al.*, 2000; Chang *et al.*, 2005; Xu *et al.*, 2006). As the main phytochemicals, diterpenoids have shown antimicrobial, antioxidant, anti-inflammatory, cytotoxic, neuroprotective, and cardioprotective effects (Li *et al.*, 2018). Sapriearine (Fig. 1A) is one of the diterpenoids found in *Salvia prionitis* (Chen *et al.*, 2002). However, to the best of our knowledge, there are no reports on its activity. In our interest to find bioactive phytochemicals for the treatment of myocardial infarction, we have investigated the protective effects of sapriearine using H9c2 cardiomyocytes induced by hypoxia/reoxygenation.

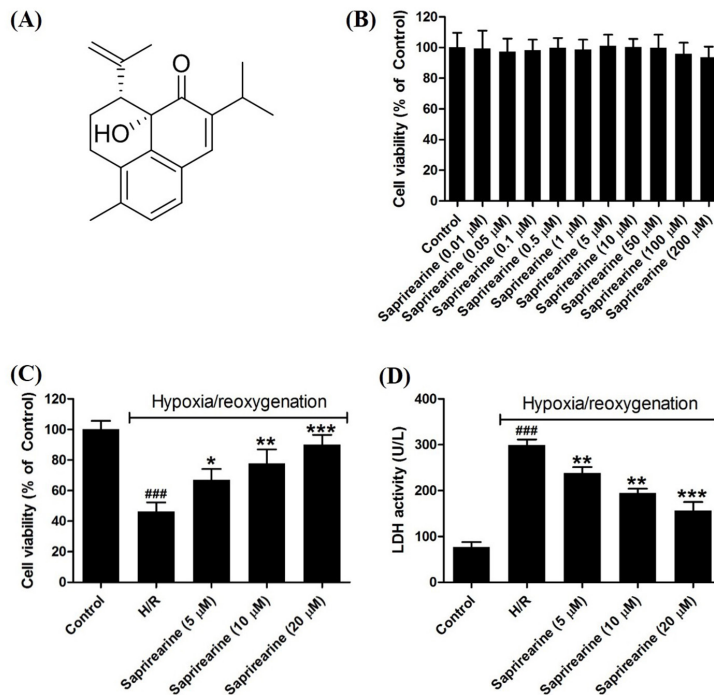


**Figure 1. Effects of sapirrearine on the survival of H9c2 cardiomyocytes.**

(A) Chemical structure of sapirrearine. (B) MTT assay for the cell viability of normal H9c2 cardiomyocytes. (C) MTT assay for cell viability of H9c2 cardiomyocytes injured by hypoxia/reoxygenation with or without sapirrearine. (D) Extracellular LDH activity in H9c2 cardiomyocytes induced by hypoxia/reoxygenation in the presence or absence of sapirrearine. Data were expressed as means  $\pm$  standard deviation,  $n=3$ , ### $P<0.001$  vs. control group, \* $P<0.05$ , \*\* $P<0.01$ , and \*\*\* $P<0.001$  vs H/G group.

## MATERIALS AND METHODS

### Chemicals and reagents

Sapirrearine was provided by Qincheng Biotechnology (Shanghai, China) with purity of more than 98% analyzed by HPLC. Dulbecco's modified Eagle's medium (DMEM) and fetal bovine serum were obtained from Invitrogen Gibco Co. (Grand Island, NY). 3-[4,5-dimethylthiazol-2-yl]-2,5-diphenyltetrazolium bromide (MTT) and dimethyl sulfoxide (DMSO) were purchased from Sigma-Aldrich (St. Louis, MO). Fluo-3 AM, ROS assay kit, lactate dehydrogenase (LDH) activity assay kit, bicinchoninic acid (BCA) protein assay kit, SOD activity assay kit, CAT activity assay kit, malondialdehyde (MDA) assay kit, mitochondrial membrane potential assay kit with JC-1 and horseradish peroxidase conjugated secondary antibody together with enhanced chemiluminescence (ECL) assay kit were provided by Beyotime Biotechnology Institute (Shanghai, China). The primary antibody for cysteinyl aspartate specific proteinase-3 cleaved (caspase-3) (#9661) was supplied by Cell Signaling Technology (Danvers, MA), and others, including B-cell lymphoma-2 (Bcl-2) (ab196495), Bcl-2-associated X protein (Bax) (ab32503) Nrf2 (ab92946),  $\beta$ -actin (ab8226) and lamin B1 (ab16048) were obtained from Abcam (Cambridge, UK). Calcein-AM was purchased from Dojindo Laboratories (Kumamoto, Japan). The ARE-luciferase reporter plasmid (pGL4.37[luc2P/ARE/Hygro]) (E3641), the renilla luciferase reporter plasmid (pRL-TK) (E2241) and the dual luciferase reporter assay system (E1910) were supplied by Promega (Madison, WI). Lipofectamine 2000 and sulforaphane were supplied by Thermo Fisher Scientific (Waltham, MA). Negative control siRNA (NC-siRNA) (sc-37007)

and Nrf2-siRNA (sc-156128) were obtained from Santa Cruz Biotechnology (Dallas, TX).

### Cell culture and treatment

Rat H9c2 cardiomyocytes were supplied by the American Type Culture Collection (ATCC, Manassas, VA) and kept in DMEM, including 10% fetal bovine serum, 100 U/mL penicillin, and 100  $\mu$ g/mL streptomycin in humid conditions with 5% CO<sub>2</sub> and 95% air at 37°C. The cells were divided into control group, hypoxia/reoxygenation (HR) group, and experimental groups. Cells in experimental groups were pretreated with certain sapirrearine or sulforaphane for 24 h and then exposed to a humid atmosphere with 95% N<sub>2</sub> and 5% CO<sub>2</sub> at 37°C for 3 h followed by reoxygenation at 37°C in 5% CO<sub>2</sub> and 95% air for another 3 h. Cells in the HR group were just subjected to hypoxia/reoxygenation without treatment with sapirrearine or sulforaphane while normoxic control cells were incubated at 37°C in 5% CO<sub>2</sub> and 95% air.

### Cell viability

Cell viability was detected using the MMT assay. Briefly, cells were seeded in 96-well microplates and treated as previously, then 20  $\mu$ L MTT (5 mg/mL) was added to each well and incubation was carried out at 37°C for 4 h. Subsequently, 100  $\mu$ L DMSO was added to dissolve the formazan crystals. The absorbance was recorded on a microplate reader (Bio-Rad, Hercules, CA) at 570 nm.

### LDH release

To further assess the damage to H9c2 cardiomyocytes, LDH release was evaluated here using the commercially available kit. The treated cells were centrifuged at 400 $\times$ g for 5 min and then the supernatant was collected and

handled according to the manufacturer's instructions. Finally, the absorbance was measured on a microplate reader at 450 nm.

### Intracellular calcium level

Intracellular calcium in H9c2 cardiomyocytes was detected using the fluorescence dye Fluo-3 AM. Following the supplier's protocol, treated cells were loaded in the dark with 5  $\mu$ M Fluo-3 AM at 37°C for 30 min, then washed with PBS three times to remove excessive dye. Fluo-3 AM can react with calcium to produce calcium-chelated Fluo-3, which can emit fluorescence at 525 nm after excited at 488 nm. The fluorescence intensity was read on a fluorescence microplate reader (Molecular Devices, Sunnyvale, CA).

### Mitochondrial membrane potential

The mitochondrial membrane potential of H9c2 cardiomyocytes was monitored using the JC-1 assay kit. Following the manufacturer's instructions, the treated H9c2 cardiomyocytes were incubated with JC-1 at 37°C for 20 min in the dark. Then the fluorescence intensity was read on a fluorescence microplate reader at 488 nm/530 nm as an excitation/emission wavelength.

### Mitochondrial permeability transition pore

To explore the mitochondrial permeability transition pore, calcein-AM was used. Briefly, treated H9c2 cardiomyocytes were incubated with 2  $\mu$ M calcein-AM and 1 mM  $\text{CoCl}_2$  at room temperature for 30 min. After removing free calcein-AM and  $\text{CoCl}_2$ , cells were incubated with  $\text{CoCl}_2$  for another 20 min at 37°C to quench the fluorescence of cytosolic calcein. The fluorescence intensity of mitochondrial calcein in cardiomyocytes was recorded on a fluorescence microplate reader at 490 nm for excitation and 515 nm for emission. The loss of calcein fluorescence in cardiomyocytes indicated the opening of the mitochondrial permeability transition pore.

### Generation of intracellular ROS

The generation of intracellular ROS was monitored by the fluorescence method using a ROS assay kit. After treatment, the medium was replaced and the cells were rinsed with PBS. Then 10  $\mu$ M DCFH-DA in DMEM was loaded and incubation was carried out at 37°C for 30 min. After being washed with PBS to remove excess dye, the fluorescence intensity was recorded on a fluorescence microplate reader at ex/em wavelength of 485/520 nm.

### MDA content

The content of MDA in H9c2 cardiomyocytes was detected using the thiobarbituric acid-based assay kit. The treated cells were lysed on ice and centrifuged at 1600 $\times$ g for 10 min. The supernatant was collected and treated according to the manufacturer's instructions. The absorbance was recorded on a microplate reader at 532 nm.

### Activity of SOD and CAT

The activity of SOD and CAT in H9c2 cardiomyocytes was assessed using the assay kits. For CAT activity, the treated cells were centrifuged and the supernatant was collected. After being treated according to the supplier's instructions, the absorbance was recorded at 520 nm. For SOD activity, the treated cells were lysed on ice

and the supernatant was collected after centrifugation. After treatment following the supplier's instructions, the absorbance was read at 560 nm.

### Immunofluorescence staining

To localize Nrf2 in H9c2 cardiomyocytes, immunofluorescence staining was employed. Cells were seeded in 12-well microplates with a coverlip and treated as above. The cells on the coverslips were then washed and fixed using a fixation mixture (acetone:methanol = 1:1) for 10 min. Then the primary Nrf2 antibody (diluted in 10% FBS-PBS) was added to the coverlip and the incubation was carried out at 4°C overnight. After washing, cells were exposed to Alex-594 conjugated secondary antibody (diluted in 10% FBS-PBS) in the dark for 1 h. The cells were then stained with DAPI in the dark for 10 min. The images were captured using a fluorescence microscope (Olympus, Tokyo, Japan).

### Proteins extraction

Total and nuclear proteins in H9c2 cardiomyocytes were extracted using the RIPA lysis buffer solution or the nuclear and cytoplasmic protein extraction kit according to the supplier's instructions. The treated cells were lysed on ice with RIPA buffer for 3 min and then centrifuged at 10000 $\times$ g for 5 min. The supernatant was collected as total proteins. For nuclear protein extraction, treated cells were exposed to 200  $\mu$ L buffer solution A containing 1 mM PMFS. After vortex for 5 s and incubation on ice for 15 min, 10  $\mu$ L buffer solution B was added. After vortex and incubation, centrifugation was carried out at 16000 $\times$ g and 4°C for 5 min. The supernatant was then removed. And the pellet was incubated with 50  $\mu$ L nuclear protein extraction solution containing PMSF on ice for 30 min. Meanwhile, the vortex was performed for 30 s every 2 min. After centrifugation, the supernatant was collected as nuclear proteins.

### Western blot analysis

After quantification using the BCA protein assay kit, the proteins were separated on 10% SDS-PAGE and then transferred to PVDF membranes. After blocking with defatted milk, the membranes were incubated with primary antibodies including cleaved caspase-3 (1:1000), Bcl-2 (1:1000), Bax (1:1000), Nrf2 (1:1000),  $\beta$ -actin (1:1000) and lamin B1 (1:1000) at 4°C overnight. The membranes were incubated with horseradish peroxidase-conjugated secondary antibodies at room temperature for 1 h and visualized using an ECL substrate on a Bio-Rad imaging system (Hercules, CA).  $\beta$ -actin and lamin B1 were used as an internal control. Densitometric analysis was performed using ImageJ software (NIH, Bethesda, MD).

### Dual luciferase reporter gene assay

The H9c2 cardiomyocytes were transfected with the ARE luciferase plasmid and the renilla luciferase plasmid using lipofectamine 2000. The cells were then treated as above and the activities of fireflies and renilla luciferase were determined by the dual luciferase reporter gene assay system. Firefly luciferase activity was normalized to renilla luciferase activity, and the induction of ARE luciferase activity was determined as a ratio compared to the control group.

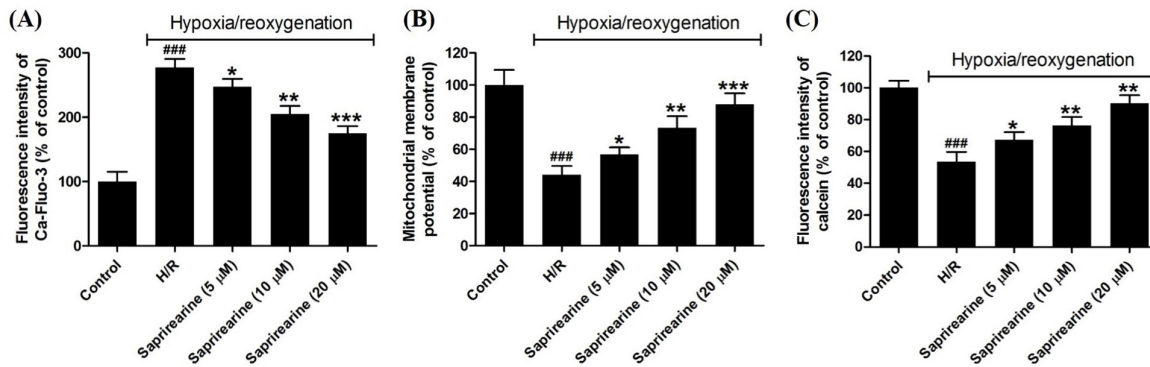


**Figure 2. Effects of sapirrearine on mitochondrial function of H9c2 cardiomyocytes induced by hypoxia/reoxygenation.**

(A) The intracellular calcium level derived from the fluorescence intensity of calcium-chelated Fluo-3 was elevated by hypoxia/reoxygenation in H9c2 cardiomyocytes and reduced by sapirrearine. (B) The mitochondrial membrane potential in H9c2 cardiomyocytes collapsed in H9c2 cardiomyocytes induced by hypoxia/reoxygenation and reversed by sapirrearine. (C) The transition pore opening of mitochondrial permeability derived from the fluorescence intensity of calcein in H9c2 cardiomyocytes was enhanced under hypoxia/reoxygenation and attenuated by sapirrearine. Data were expressed as means  $\pm$  standard deviation,  $n=3$ ,  $^{###}P<0.001$  vs control group,  $^{*}P<0.05$ ,  $^{**}P<0.01$ , and  $^{***}P<0.001$  vs H/G group.

### SiRNA interference assay

To elucidate the role of Nrf2 in the protective effects of sapirrearine, siRNA interference was used. Cells were transfected with normal control siRNA (NC-siRNA) or Nrf2-siRNA. A western blot assay was then performed to validate whether transfection was successful. The successfully transfected cells were treated as above. And the MTT assay was used to determine cell viability.

### Statistical analysis

All experimental data were expressed as mean  $\pm$  standard deviation and analyzed with GraphPad Prism 5.0 (San Diego, CA). One-way ANOVA followed by Tukey test for multiple comparisons and Student's *t*-test for single components was implemented. It was considered significant in statistics when  $P<0.05$ .

## RESULTS

### Sapirrearine improves the survival of H9c2 cardiomyocytes induced by hypoxia/reoxygenation

As shown in Fig. 1B, up to 200  $\mu$ M there is no cytotoxic effect of sapirrearine on H9c2 cardiomyocytes. After treatment with hypoxia/reoxygenation viability was markedly reduced ( $46.3 \pm 6.0\%$ ), while in the presence of sapirrearine at 5, 10 and 20  $\mu$ M, the cell viability was elevated to  $67.0 \pm 7.2\%$ ,  $77.9 \pm 9.1\%$ , and  $90.2 \pm 6.3\%$ , respectively (Fig. 1C). Further investigation of LDH activity has revealed that hypoxia/reoxygenation resulted in increased extracellular LDH activity ( $299.2 \pm 12.4$  U/L) compared to the control group ( $77.1 \pm 10.8$  U/L). However, sapirrearine at 5, 10, and 20  $\mu$ M could significantly decrease LDH activity ( $238.1 \pm 13.0$ ,  $194.8 \pm 9.4$  and  $156.3 \pm 18.9$  U/L) (Fig. 1D).

### Sapirrearine attenuates the mitochondrial dysfunction induced by hypoxia/reoxygenation in H9c2 cardiomyocytes

To detect mitochondrial function, first the intracellular calcium level was measured using the fluorescence dye Fluo-3 AM. As a result, hypoxia/reoxygenation induced calcium overload ( $277.5 \pm 13.0\%$ ), which is much higher than the control group ( $100.0 \pm 15.2\%$ ). After exposure

to sapirrearine, calcium-induced fluorescence was reduced to  $247.4 \pm 12.3\%$ ,  $204.8 \pm 12.5\%$  and  $175.1 \pm 11.1\%$  in a dose-dependent manner (Fig. 2A). Meanwhile, the mitochondrial membrane potential was observed to collapse after hypoxia/reoxygenation treatment ( $44.2 \pm 5.5\%$ ) compared to the control group ( $100.0 \pm 11.1\%$ ). But sapirrearine at 5, 10 and 20  $\mu$ M reversed the decline of mitochondrial membrane potential ( $56.8 \pm 4.4\%$ ,  $73.3 \pm 7.3\%$  and  $88.1 \pm 6.7\%$ ) (Fig. 2B). Similarly, the opening of the mitochondrial permeability transition pore was detected under hypoxia/reoxygenation by monitoring the fluorescence intensity of mitochondrial calcein ( $53.5 \pm 6.3\%$ ), which was attenuated by sapirrearine ( $67.4 \pm 4.7\%$ ,  $76.3 \pm 5.4\%$  and  $90.3 \pm 5.1\%$ ) (Fig. 2C). These findings indicated that sapirrearine relieved mitochondrial dysfunction in H9c2 cardiomyocytes treated with hypoxia/reoxygenation.

### Sapirrearine ameliorates hypoxia/reoxygenation-induced oxidative stress in H9c2 cardiomyocytes

To reveal the redox status in cardiomyocytes, we explore intracellular ROS herein. As a result, unlike the control group ( $100.0 \pm 18.0\%$ ), overproduction was found in cardiomyocytes after hypoxia/reoxygenation induction ( $298.1 \pm 13.0\%$ ), while sapirrearine at 5, 10 and 20  $\mu$ M diminished the intracellular ROS level ( $251.4 \pm 11.6\%$ ,  $199.1 \pm 12.6\%$  and  $160.1 \pm 13.5\%$ ) (Fig. 3A). As a product of lipid peroxidation, the content of MDA has been elevated by hypoxia/reoxygenation ( $175.4 \pm 7.1\%$ ). After exposure to certain sapirrearine, the generation of MDA was suppressed as  $156.0 \pm 7.7\%$ ,  $138.7 \pm 8.2\%$  and  $123.4 \pm 7.6\%$ , respectively (Fig. 3B). At the same time, the results showed that hypoxia/reoxygenation led to inhibition of SOD ( $46.7 \pm 6.3\%$ ) and CAT ( $49.6 \pm 6.6\%$ ), while sapirrearine activated SOD ( $62.8 \pm 6.7\%$ ,  $79.2 \pm 7.6\%$  and  $90.3 \pm 5.6\%$ ) and CAT ( $64.4 \pm 5.4\%$ ,  $81.5 \pm 5.5\%$  and  $90.2 \pm 4.5\%$ ) in a dose-dependent manner (Fig. 3C and D).

### Sapirrearine inhibits the apoptosis of H9c2 cardiomyocytes induced by hypoxia/reoxygenation

Proteins related to apoptosis, including cleaved caspase-3, Bcl-2, and Bax, were analyzed by Western blot. As shown in Fig. 4A, hypoxia/reoxygenation caused the increase in cleaved caspase-3, which was repressed

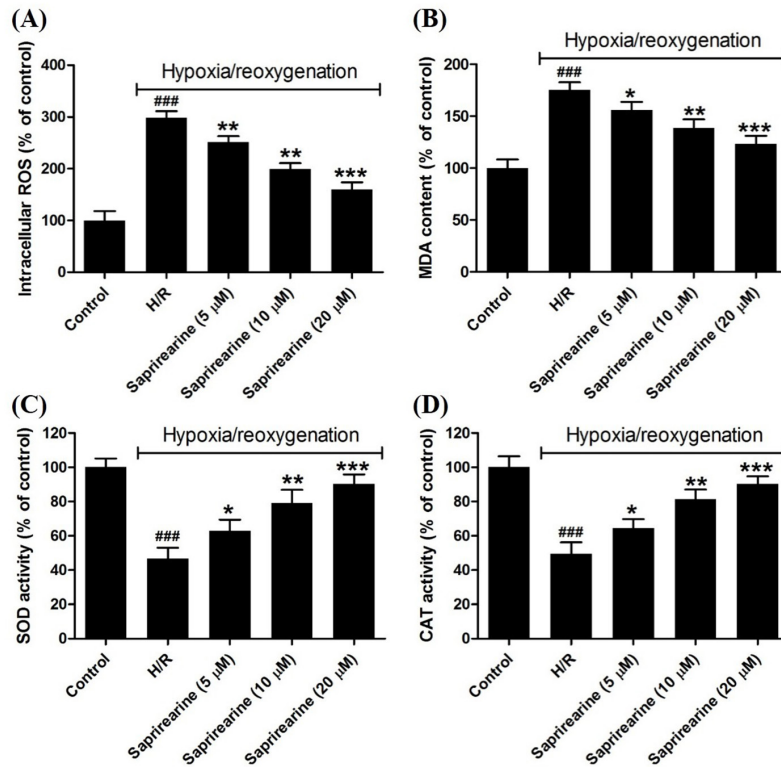


**Figure 3. Effects of sapirrearine on oxidative stress in H9c2 cardiomyocytes.**

(A) The intracellular ROS level in H9c2 cardiomyocytes was increased by hypoxia/reoxygenation and decreased by sapirrearine. (B) The MDA content in H9c2 cardiomyocytes was excessively generated by hypoxia/reoxygenation and reversed by sapirrearine. (C–D) SOD and CAT activity in H9c2 cardiomyocytes was inhibited by hypoxia/reoxygenation and activated by sapirrearine. Data were expressed as means  $\pm$  standard deviation,  $n=3$ , ### $P<0.001$  vs control group, \* $P<0.05$ , \*\* $P<0.01$ , and \*\*\* $P<0.001$  vs H/G group.

in the presence of sapirrearine. Densitometric analysis also revealed similar results (Fig. 4B). Meanwhile, anti-apoptotic Bcl-2 was up-regulated, and pro-apoptotic Bax was down-regulated after being exposed to sapirrearine (Fig. 4A). Accordingly, the ratio of Bcl2/Bax gave a clear trend for the effects of sapirrearine on cardiomyocyte apoptosis.

#### Sapirrearine activates Nrf2 in H9c2 cardiomyocytes induced by hypoxia/reoxygenation

To unravel the mechanism of sapirrearine against apoptosis of cardiomyocytes induced by hypoxia/re-

oxygenation, we have explored the activation of Nrf2. Immunofluorescence staining has indicated that sapirrearine elevated Nrf2 as well as promoted its translocation to nuclei from the cytosol (Fig. 5A). Western blot analysis together with densitometric analysis showed that sapirrearine resulted in up-regulation of nuclear Nrf2, which further implied that its translocation was promoted (Fig. 5B and C). Meanwhile, total Nrf2 was also up-regulated (Fig. 5B and D), indicating that sapirrearine improved Nrf2 stability against its degradation. Furthermore, the dual luciferase reporter assay revealed that Nrf2 binding capacity to ARE

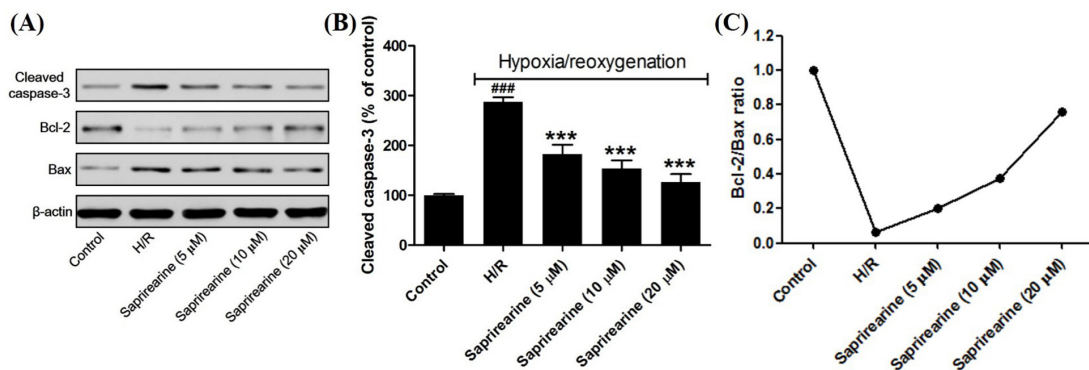


**Figure 4. Effects of sapirrearine on apoptosis of H9c2 cardiomyocytes induced by hypoxia/reoxygenation.**

(A) Western blot analysis of proteins related to apoptosis in H9c2 cardiomyocytes induced by hypoxia/reoxygenation with or without sapirrearine. (B) Densitometric analysis of cleaved caspase-3 in H9c2 cardiomyocytes induced by hypoxia/reoxygenation with or without sapirrearine. (C) Relative ratio of Bcl-2/Bax in H9c2 cardiomyocytes. Data were expressed as means  $\pm$  standard deviation,  $n=3$ , ### $P<0.001$  vs control group, \*\*\* $P<0.001$  vs H/G group.

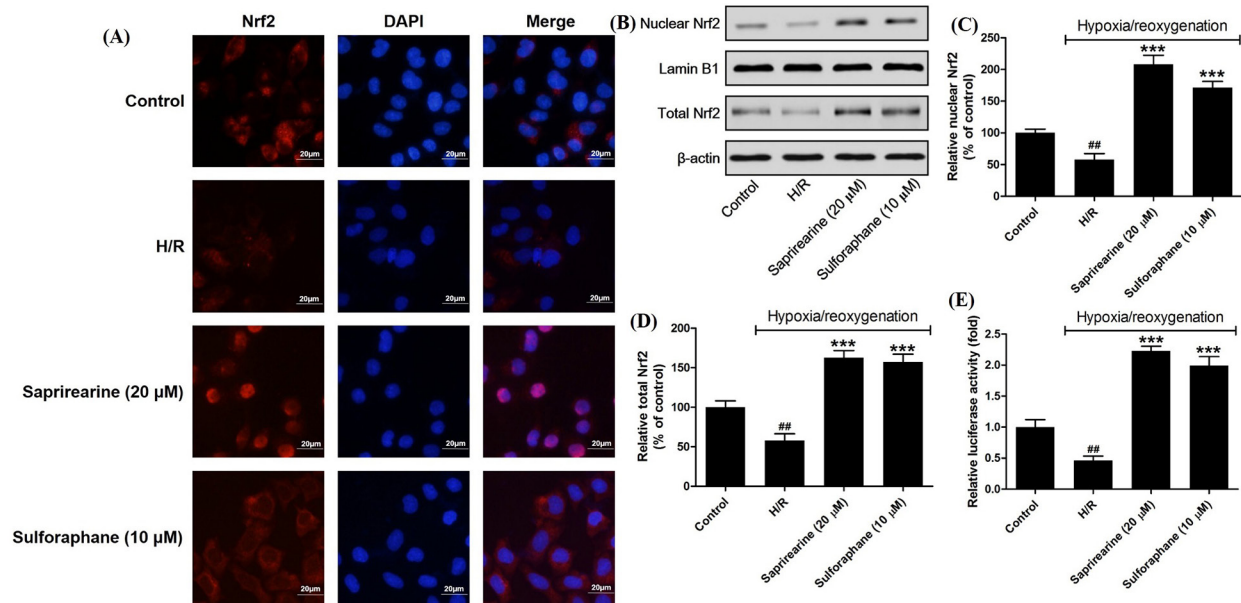


**Figure 5. Effects of sapirearine on Nrf2 activation in H9c2 cardiomyocytes.**

(A) Immunofluorescence staining for Nrf2 in H9c2 cardiomyocytes induced by hypoxia/reoxygenation. (B) Western blot analysis for nuclear and total Nrf2 in H9c2 cardiomyocytes injured by hypoxia/reoxygenation with or without sapirearine. (C–D) Densitometric analysis for nuclear and total Nrf2. (E) Dual luciferase reporter assay for the ability of Nrf2 to bind to ARE in H9c2 cardiomyocytes induced by hypoxia/reoxygenation in the presence or absence of sapirearine. Data were expressed as means  $\pm$  standard deviation,  $n=3$ ,  $^{**}P<0.01$  vs control group,  $^{***}P<0.001$  vs H/G group.

was significantly improved to regulate transcription after treatment with sapirearine (Fig. 5E). Collectively, these observations revealed sapirearine-activated Nrf2 in H9c2 cardiomyocytes.

#### Nrf2 activation is involved in the protective effects of sapirearine

To clarify the role of Nrf2 activation in the protective effects of sapirearine, siRNA interference was performed. After transfected with NC-siRNA or Nrf2-siRNA, Western blot together with densitometric analysis has validated that transfection was successfully (Fig. 6A and B). Then the MTT was implemented. As shown in Fig. 6C, in H9c2 cardiomyocytes transfected with NC-siRNA, sapirearine was observed to promote cell viability, while in cells transfected with Nrf2-siRNA, sapirearine did not enhance cell viability (Fig. 6C). These results demonstrated that sapirearine protected H9c2 cardiomyocytes against hypoxia/reoxygenation-induced injury by activating Nrf2.

#### DISCUSSION

Myocardial infarction remains the leading cause of mortality and disability worldwide. As primary treatment, timely reperfusion itself causes major cardiac injury, commonly referred to as myocardial ischemia/reperfusion injury (Zhao *et al.*, 2016). Therefore, the discovery of novel therapy targeting myocardial ischemia/reperfusion is imperative. Here, we have found that sapirearine improved the survival of hypoxia/reoxygenation-induced H9c2 cardiomyocytes by increasing cell viability and inhibiting intracellular LDH release.

In the pathogenesis of myocardial ischemia/reperfusion injury, oxidative stress plays a crucial role due to the overproduction of ROS in reperfusion (Loor *et al.*, 2011). To reduce molecular oxygen, enzymes such as xanthine oxidase and NADPH oxidase, as well as the mitochondrial electron transport chain in reperfusion myocardial tissue, will accelerate ROS production (Granger & Kvietys, 2015). As one of ROS, superoxide is generated from one electron reduction of molecular oxygen

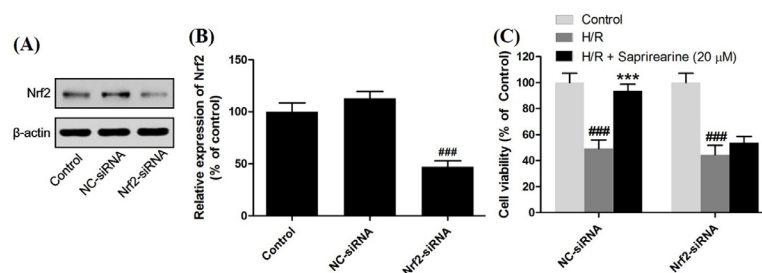


**Figure 6. Nrf2 activation is involved in the protective effects of sapirearine.**

(A) Western blot analysis of Nrf2 in H9c2 cardiomyocytes transfected with NC-siRNA or Nrf2-siRNA. (B) Densitometric analysis of Nrf2. (C) Cell viability of H9c2 cardiomyocytes transfected with NC-siRNA or Nrf2-siRNA and induced by hypoxia/reoxygenation with or without sapirearine. Data were expressed as means  $\pm$  standard deviation,  $n=3$ ,  $^{###}P<0.001$  vs control group,  $^{***}P<0.001$  vs H/G group.

and converted to hydrogen peroxide by SOD, which is decomposed as water under the catalysis of CAT (Dickinson & Chang, 2011). In the present investigations, hypoxia/reoxygenation was observed to promote the overproduction of ROS and MDA in H9c2 cardiomyocytes. Meanwhile, the activity of SOD and CAT was inhibited. This poor oxidative state was reversed in the presence of sapirrearine.

As the main site of ROS production, mitochondria are sensitive to ROS-related injury (Brand, 2016). Following ROS overproduction, calcium overloads as an important second messenger due to its interaction (Görlach *et al.*, 2015). In ischemia reperfusion injury, calcium promotes the opening of the mitochondrial permeability transition pore (Hurst *et al.*, 2017). When the mitochondrial permeability transition pore opens, its large conductance can result in collapse of the mitochondrial membrane potential as the early event of apoptosis (Halestrap, 2010). Meanwhile, the poor potential of the mitochondrial membrane affects the influx of mitochondrial calcium and leads to the release of calcium into the cytosol (Hausenloy & Yellon, 2013). From current studies, sapirrearine was found to inhibit calcium release, attenuated the collapse of the mitochondrial membrane, and suppressed the opening of the mitochondrial membrane permeability transition pore induced by hypoxia/reperfusion.

In apoptosis, caspases play a central role as cysteinyl aspartate specific proteinase, which are activated by cleavage at specific sites (Budihardjo *et al.*, 1999). Of the caspases, caspase-3 is the key effector enzyme closely associated with cell apoptosis and morphological changes (Uchiyama *et al.*, 2002). Bcl-2 and Bax are members of the Bcl-2 protein family and participate in mitochondrial-mediated apoptosis. Bcl-2 inhibits apoptosis and inactivates caspase-3, while Bax promotes cell apoptosis (Youle & Strasser, 2008). The formation of heterodimers with Bcl-2 and Bax prevents the oligomerization of Bax which will trigger the apoptotic cascade (Ola *et al.*, 2011). In our investigations, the results showed that sapirrearine inhibited the activation of caspase-3, up-regulated Bcl-2, and down-regulated Bax, which implied that it repressed apoptosis of H9c2 cardiomyocytes induced by hypoxia/reoxygenation.

As a transcription factor, Nrf2 enhances the expression of genes that encode antioxidant enzymes (Cuadrado *et al.*, 2018). Structural analysis of the Keap1-Nrf2 complex has indicated that the Keap1 homodimer interacts with the DLG and ETGE motifs of Nrf2 using their Kelch domains, respectively, which results in the retention of Nrf2 in the cytosol (Madden & Itzhaki, 2020). Due to the lower affinity for binding for binding of DLG to Kelch compared to ETGE, the complex forms a “hinge and latch” model (Tong *et al.*, 2007). Oxidants or electrophiles can react with thiol groups in Keap1 cysteine residues through the formation of covalent bonds to alter Keap1 formation and lead to the dissociation of DLG from Keap1 (Yamamoto *et al.*, 2008). Therefore, this interaction could prevent the ubiquitination and degradation of Nrf2 involving Keap1. Michael acceptors are typical electrophiles such as soft Lewis acids, which can react with critical cysteine thiolate (soft base) groups in Keap1 through the Michael addition reaction (Magesh *et al.*, 2012). From the structure of sapirrearine, we can find the coumaroyl moiety, which may indicate that it can activate Nrf2. In our investigations, Nrf2 is activated by sapirrearine in H9c2 cardiomyocytes, which is closely associated with its protective effects against hypoxia/reoxygenation-induced apoptosis.

## CONCLUSION

In conclusion, we have evaluated the protective effects of sapirrearine against hypoxia/reoxygenation-induced apoptosis using H9c2 cardiomyocytes and explored the underlying mechanisms. The results showed that sapirrearine could protect hypoxia/reoxygenated H9c2 cardiomyocytes against mitochondria-mediated apoptosis by inhibiting oxidative stress and improving mitochondrial dysfunction. And activation of Nrf2 was involved in those protective effects. These findings can provide evidence for the discovery of new therapeutic approaches to myocardial infarction and the application of sapirrearine in clinical practice.

## REFERENCES

- Brand MD (2016) Mitochondrial generation of superoxide and hydrogen peroxide as the source of mitochondrial redox signaling. *Free Radical Biol Med* **100**: 14–31. <https://doi.org/10.1016/j.freeradbiomed.2016.04.001>
- Budihardjo I, Oliver H, Lutter M, Luo X, Wang X (1999) Biochemical pathways of caspase activation during apoptosis. *Annu Rev Cell Dev Biol* **15**: 269–290. <https://doi.org/10.1146/annurev.cellbio.15.1.269>
- Chang J, Xu J, Li M, Zhao M, Ding J, Zhang JS (2005) Novel cytotoxic *seco*-abietane rearranged diterpenoids from *Salvia prionitis*. *Planta Med* **71**: 861–866. <https://doi.org/10.1055/s-2005-871279>
- Chen X, Ding J, Ye YM, Zhang JS (2002) Bioactive abietane and *seco*-abietane diterpenoids from *Salvia prionitis*. *J Nat Prod* **65**: 1016–1020. <https://doi.org/10.1021/np010561j>
- Cuadrado A, Manda G, Hassan A, Alcaraz MJ, Barbas C, Daiber A, Ghezzi P, León R, López MG, Oliva B, Pajares M, Rojo AI, Robledinos-Antón N, Valverde AM, Guney E, Schmidt HHHW (2018) Transcription factor NRF2 as a therapeutic target for chronic diseases: a systems medicine approach. *Pharmacol Rev* **70**: 348–383. <https://doi.org/10.1124/pr.117.014753>
- Dickinson BC, Chang CJ (2011) Chemistry and biology of reactive oxygen species in signaling or stress responses. *Nat Chem Biol* **7**: 504–511. <https://doi.org/10.1038/nchembio.607>
- Görlach A, Bertram K, Hudecov S, Krizanova O (2015) Calcium and ROS: a mutual interplay. *Redox Biol* **6**: 260–271. <https://doi.org/10.1016/j.redox.2015.08.010>
- Granger DN, Kvietys PR (2015) Reperfusion injury and reactive oxygen species: the evolution of a concept. *Redox Biol* **6**: 524–551. <https://doi.org/10.1016/j.redox.2015.08.020>
- Halestrap AP (2010) A pore way to die: the role of mitochondria in reperfusion injury and cardioprotection. *Biochem Soc Trans* **38**: 841–860. <https://doi.org/10.1016/10.1042/BST0380841>
- Hausenloy DJ, Yellon DM (2013) Myocardial ischemia-reperfusion injury: a neglected therapeutic target. *J Clin Invest* **123**: 92–100. <https://doi.org/10.1172/JCI62874>
- Hurst S, Hoek J, Sheu SS (2017) Mitochondrial Ca<sup>2+</sup> and regulation of the permeability transition pore. *J Bioenerg Biomembr* **49**: 27–47. <https://doi.org/10.1007/s10863-016-9672-x>
- Kaspar JW, Nitire SK, Jaiswal AK (2009) Nrf2:INrf2 (Keap1) signaling in oxidative stress. *Free Radic Biol Med* **47**: 1304–1309. <https://doi.org/10.1016/j.freeradbiomed.2009.07.035>
- Kumar M, Nayak PK (2017) Natural phytochemicals: a promising approach in the management of myocardial infarction. *Biomed Pharmacother* **92**: 1138–1139. <https://doi.org/10.1016/j.biopha.2016.12.139>
- Li L, Zhou M, Xue G, Wang W, Zhou X, Wang X, Kong L, Luo J (2018) Bioactive *seco*-abietane rearranged diterpenoids from the aerial parts of *Salvia prionitis*. *Bioorg Chem* **81**: 454–460. <https://doi.org/10.1016/j.bioorg.2018.08.040>
- Li M, Zhang JS, Ye YM, Fang JN (2000) Constituents of the roots of *Salvia prionitis*. *J Nat Prod* **63**: 139–141. <https://doi.org/10.1021/np990357k>
- Loor G, Kondapalli J, Iwase H, Chandel NS, Waypa GB, Guzy RD, Vanden Hoek TL, Schumacker PF (2011) Mitochondrial oxidant stress triggers cell death in simulated ischemia-reperfusion. *Biochim Biophys Acta* **1813**: 1382–1394. <https://doi.org/10.1016/j.bbamcr.2010.12.008>
- Madden SK, Itzhaki LS (2020) Structural and mechanistic insights into the Keap1-Nrf2 system as a route to drug discovery. *Biochim Biophys Acta Proteins Proteom* **1868**: 140405. <https://doi.org/10.1016/j.bbapap.2020.140405>
- Magesh S, Chen Y, Hu L (2012) Small molecule modulators of Keap1-Nrf2-ARE pathway as potential preventive and therapeutic agents. *Med Res Rev* **32**: 687–726. <https://doi.org/10.1002/med.21257>
- Marczin N, El-Habashi N, Hoare GS, Bundy RE, Yacoub M (2003) Antioxidants in myocardial ischemia-reperfusion injury: therapeutic

- potential and basic mechanisms. *Arch Biochem Biophys* **420**: 222–236. <https://doi.org/10.1016/j.abb.2003.08.037>
- Ola MS, Nawaz M, Ahsan H (2011) Role of Bcl-2 family proteins and caspases in the regulation of apoptosis. *Mol Cell Biochem* **351**: 41–58. <https://doi.org/10.1007/s11010-010-0709-x>
- Shaw P, Chattopadhyay A (2020) Nrf2-ARE signaling in cellular protection: mechanism of action and the regulatory mechanisms. *J Cell Physiol* **235**: 3119–3130. <https://doi.org/10.1002/jcp.29219>
- Shen Y, Liu X, Shi J, Wu X (2019) Involvement of Nrf2 in myocardial ischemia and reperfusion injury. *Int J Biol Macromol* **125**: 496–502. <https://doi.org/10.1016/j.ijbiomac.2018.11.190>
- Thygesen K, Alpert JS, Jaffe AS, Simoons ML, Chaitman BR, White HD, Task Force for the Universal Definition of Myocardial Infarction (2012) Third universal definition of myocardial infarction. *Nat Rev Cardiol* **9**: 620–633. <https://doi.org/10.1038/nrcardio.2012.122>
- Tong KI, Padmanabhan B, Kobayashi A, Shang C, Y. Hirotsu, Yokoyama S, Yamamoto M (2007) Different electrostatic potentials define ETGE and DLG motifs as hinge and latch in oxidative stress response. *Mol Cell Biol* **27**: 7511–7521. <https://doi.org/10.1128/MCB.00753-07>
- Uchiyama T, Otani H, Okada T, Ninomiya H, Kido M, Imamura H, Nogi S, Kobayashi Y (2002) Nitric oxide induces caspase-dependent apoptosis and necrosis in neonatal rat cardiomyocytes. *J Mol Cell Cardiol* **34**: 1049–1061. <https://doi.org/10.1006/jmcc.2002.2045>
- Xu J, Chang J, Zhao M, Zhang JS (2006) Abietane diterpenoid dimers from the roots of *Salvia prionitis*. *Phytochemistry* **67**: 795–799. <https://doi.org/10.1016/j.phytochem.2005.12.023>
- Xu J, Wei K, Zhang G, Lei L, Yang D, Wang W, Han Q, Xia Y, Bi Y, Yang M, Li M (2018) Ethnopharmacology, phytochemistry, and pharmacology of Chinese *Salvia* species: a review. *J Ethnopharmacol* **225**: 18–30. <https://doi.org/10.1016/j.jep.2018.06.029>
- Yamamoto T, Suzuki T, Kobayashi A, Wakabayashi J, Maher J, Motohashi H, M. Yamamoto H (2008) Physiological significance of reactive cysteine residues of Keap1 in determining Nrf2 activity. *Mol Cell Biol* **28**: 2758–2770. <https://doi.org/10.1128/MCB.01704-07>
- Yamamoto M, Kensler TW, Motohashi H (2018) The KEAP1-NRF2 system: a thiol-based sensor-effector apparatus for maintaining redox homeostasis. *Physiol Rev* **98**: 1169–1203. <https://doi.org/10.1152/physrev.00023.2017>
- Yellon DM, Hausenloy DJ (2007) Myocardial Reperfusion Injury. *N Engl J Med* **357**: 1121–1135. <https://doi.org/10.1056/NEJMr071667>
- Youle RJ, Strasser A. (2008) The BCL-2 protein family: opposing activities that mediate cell death. *Nat Rev Mol Cell Biol* **9**: 47–59. <https://doi.org/10.1038/nrm2308>
- Zhao GL, Yu LM, Gao WL, Duan WX, Jiang B, Liu XD, Zhang B, Liu ZH, Zhai ME, Jin ZX, Yu SQ, Wang Y (2016) Berberine protects rat heart from ischemia/reperfusion injury via activating JAK2/STAT3 signaling and attenuating endoplasmic reticulum stress. *Acta Pharmacol Sin* **37**: 354–367. <https://doi.org/10.1038/aps.2015.136ol>
- Zhao LM, Liang XT, Li LN (1996) Prionitisides A and B, two phenolic glycosides from *Salvia prionitis*. *Phytochemistry* **42**: 899–901. [https://doi.org/10.1016/0031-9422\(95\)00967-1](https://doi.org/10.1016/0031-9422(95)00967-1)
- Zhao ZQ (2004) Oxidative stress-elicited myocardial apoptosis during reperfusion. *Curr Opin Pharmacol* **4**: 159–165. <https://doi.org/10.1016/j.coph.2003.10.010>